



Pathogen-induced defoliation impacts on transpiration, leaf gas exchange, and non-structural carbohydrate allocation in eastern white pine (*Pinus strobus*)

Cameron D. McIntire^{1,2} · Brett A. Huggett³ · Emma Dunn³ · Isabel A. Munck¹ · Matthew A. Vadeboncoeur⁴ · Heidi Asbjornsen^{2,4}

Received: 11 August 2019 / Accepted: 18 September 2020 / Published online: 10 October 2020
© Springer-Verlag GmbH Germany, part of Springer Nature 2020

Abstract

Key message Pathogen-induced defoliation resulted in a reduction in transpiration, an upregulation of photosynthesis in the early growing season, and no change in NSC reserves across stem, root, and foliar tissues.

Abstract The defoliation of eastern white pine (*Pinus strobus* L.) by native fungi associated with white pine needle damage (WPND) can substantially reduce foliar area for much of the growing season in the northeastern United States. Chronic defoliations in the region are known to have slowed growth rates in symptomatic stands, but the physiological impacts of WPND as it relates to tree water use and carbon assimilation are largely unresolved. We investigated how the severity of WPND defoliation influences transpiration throughout the course of a growing season. We also assessed leaf-level gas exchange between defoliation severity classes and needle age over time. Finally, we compared concentrations of non-structural carbohydrates (NSC) between defoliation severity classes in five different tissue types over time. We found that trees experiencing a high-severity defoliation had 20% lower sap flux density compared to low-severity individuals. We found that rates of photosynthesis were significantly influenced by the needle age class and time of year, while instantaneous water use efficiency was higher across all needle age classes late in the growing season. Our findings suggest that the residual current-year foliage of high-severity defoliated trees compensated for the loss of mature second- and third-year foliage in the early portion of the growing season. This study found that soluble sugars and starch varied significantly over time and by tissue type, but defoliation severity had little effect on NSC concentrations. Together with reduced basal area increment in high-severity trees relative to low-severity trees, this indicates that WPND-affected trees are prioritizing NSC storage over secondary growth.

Keywords White pine needle damage · Defoliation · Forest pathogen · Sap flux · Leaf gas exchange · Non-structural carbohydrates

Communicated by Jared LeBoldus.

Electronic supplementary material The online version of this article (<https://doi.org/10.1007/s00468-020-02037-z>) contains supplementary material, which is available to authorized users.

✉ Cameron D. McIntire
cameron.mcintire@usda.gov

¹ Present Address: USDA Forest Service, State and Private Forestry, 271 Mast Rd., Durham, NH, USA

² Department of Natural Resources and the Environment, University of New Hampshire, 56 College Rd., Durham, NH, USA

Introduction

Defoliation of eastern white pine (*Pinus strobus* L.) by pathogens associated with white pine needle damage (WPND) has become a chronic forest health issue throughout the northeastern United States in recent years (Broders

³ Department of Biology, Bates College, 2 Andrews Rd., Lewiston, ME, USA

⁴ Earth Systems Research Center, University of New Hampshire, 8 College Rd., Durham, NH, USA

et al. 2015; Costanza et al. 2018; Munck et al. 2012). The four ascomycete fungal pathogens which are presently associated with WPND are *Lecanosticta acicola* Thümen, *Lophophacidium dooksii* Corlett and Shoemaker, *Bifusella linearis* Peck, and *Septorioides strobi* Wyka and Broders. Each of these causal agents are considered to be native to the northeastern US and induce symptoms of chlorosis in mature needles in the late spring, followed by a defoliation of infected foliage. The establishment and persistence of WPND in the region is thought to be tightly linked with climate; notably the trend of warmer-than-average springs coupled with the increasing frequency of precipitation (Wyka et al. 2017, 2018a). Needle casting occurs primarily in the months of June through July, resulting in a 25–73% decline in stem basal area increment compared to pre-outbreak growth trends (McIntire et al. 2018a; Wyka et al. 2018b). Presently, there are no published data on the physiological impacts on WPND-induced defoliation on eastern white pine as it relates to carbon (C) assimilation, C allocation, and water use within infected stands.

Water used through transpiration is necessary for physiological processes such as photosynthesis and nutrient uptake that are essential for maintaining plant life. The recurrent summer defoliations induced by WPND in recent years significantly reduce total leaf area of infected trees and have been observed to coincide with the premature dieback of branches within the lower crown, resulting in a reduction of live crown ratios (McIntire et al. 2018b). Trees defoliated by WPND are lacking much of their mature second- and third-year foliage for the remainder of the growing season, subsisting principally on the current-year needles for maintaining crown conductance. Due to this loss of functional foliar area, diseased individuals will presumably experience a reduction in water use and gross carbon assimilation corresponding to the severity of defoliation. Such a response has been measured in *Tamarix* species defoliated by the saltcedar beetle (*Diorhabda carinulata*), in which episodic partial defoliation resulted in a 16% reduction in mean annual sap flux density (Hultine 2010). However, the relationship between foliar area, leaf gas exchange, and sap flux is complex, as leaf-level compensatory responses have shown to increase stomatal conductance and transpiration in some cases (Damascos et al. 2005; Meinzer and Grantz 1991; Pataki et al. 1998; Reich et al. 1993; Williams et al. 2016). This upregulation of gas exchange and transpiration is not consistent across tree species or among different classes of defoliator (e.g. insect, pathogen, and artificial) and, therefore, warrants additional research to better understand how reductions in leaf area influence water use and productivity over the course of a growing season. Moreover, defoliation-induced alterations in photosynthesis and stomatal conductance may also have significant implications for water use efficiency (WUE) and, in turn, the ability to respond to climate variability.

The dynamics of non-structural carbohydrates (NSC) within the context of defoliation are also highly complex. Trees utilize NSC readily for metabolism and growth, and can potentially store them for years (Richardson et al. 2015). It has been suggested that C allocation priority is first designated to facilitate short-term survival, and then utilized for processes that support long-term fitness (i.e., growth and reproduction), with any excess NSC either actively or passively stored (Dietze et al. 2014; Wiley and Helliker 2012). While many studies have investigated NSC allocation and storage within trees subject to either natural (Hudgeons et al. 2007; Jacquet et al. 2013; Palacio et al. 2012; Saffell et al. 2014a, b; Wargo et al. 2002) or artificial defoliation (Gómez-Gallego et al. 2020; Handa et al. 2005; Jacquet et al. 2014; Li et al. 2002; Palacio et al. 2008; Puri et al. 2015a; Wiley et al. 2013, 2016), there is no consistent response that can be assumed to occur for an emerging pathogen complex such as WPND. A subsequent decline or increase of NSC following needle loss is likely a function of defoliation severity, duration, or repetition of the defoliation event, compounded with other abiotic stressors (e.g., drought) and functional traits of the host species. In *P. strobus*, NSC have been found to have relatively fast rates of turnover and actively mix with new photosynthate (Richardson et al. 2015), and, thus, may be allocated rapidly in response to defoliation if needed. As NSC are highly mobile, the current-year foliage of conifers may be an important location for photosynthate storage, particularly when previous-year mature foliage is lost to pathogen induced defoliation. Current-year foliage has been found to have significantly lower NSC content compared to mature second-year foliage among the evergreen conifers *Abies georgei* and *Juniperus saltuaria* (Li et al. 2009), as well as *Pinus koraiensis* (Yan et al. 2012). If this relationship holds true for *P. strobus*, WPND-infected trees may be at a distinct disadvantage for the later part of the growing season once the majority of mature foliage has been lost, compromising the trees' water uptake and ability to assimilate and store carbon (Thomas and Sadras 2001).

The aims of this study were to quantify changes in tree water use, C assimilation, and NSC allocation within mature trees impacted by natural defoliation from WPND. Specifically, we (1) evaluated how tree sap flux varied between defoliation severity classes over the course of a single growing season in response to climatic drivers of transpiration; (2) compared measurements of post-defoliation leaf gas exchange (photosynthesis and instantaneous water use efficiency) in residual foliage to pre-defoliation levels; and (3) quantified NSC concentrations in healthy and symptomatic trees in five different storage pools over the course of a growing season.

Methods

Study region and site description

Physiological measurements of *P. strobus* were conducted at three field sites in Maine and New Hampshire: the Massabesic Experimental Forest in Lyman, ME (MEF; 43.567, – 70.640), the Fox State Forest in Hillsborough, NH (FOX; 43.127, – 71.908), and the University of New Hampshire's Foss Farm in Durham, NH (DUR, 43.108, – 70.952). Sites MEF and FOX are included in a regional permanent plot network in which assessments of WPND symptoms and defoliation severity are surveyed annually by the US Forest Service and state cooperators (Broders et al. 2015). Both MEF and FOX have been documented to experience WPND-induced defoliations since 2012. A nearby study site at DUR was evaluated in an initial survey of WPND in 2012 and was determined to be asymptomatic; however, sub-annual litterfall measurements from 2014 through 2016 revealed a relatively small degree of defoliation occurring in the summer months (McIntire et al. 2018a). Within each site, trees exhibit varying degrees of disease severity. Severity of WPND infection was measured in mid-June on a discrete scale using an established protocol consistent with the US Forest Service's annual survey (Broders et al. 2015). The total crown area is visually segmented into thirds, and then, chlorosis and needle retention are assessed within each segment. Trees are rated on a 0–3 scale, where 0 corresponds to a healthy crown free of signs and symptoms of WPND, 1 indicates that $\leq 1/3$ of the crown is affected, 2 indicates that $1/3 - 2/3$ of the crown is affected, and 3 infers that $\geq 2/3$ of the crown exhibits infection. Trees are referred to herein as exhibiting low and high disease severity, where low-severity trees received a rating of 0 and 1, while high-severity trees are those rated as 2 and 3. For the purposes of this study, observations of chlorosis are factored into the defoliation severity rating, as chlorotic needles are ultimately cast. It is common to find healthy/low-severity trees growing alongside diseased/high-severity trees within a stand. During the initial WPND site surveys in 2012, fungal pathogens were confirmed (*L. dooksii*, *B. linearis*, and *L. acicola*) and trees were classified in low- and high-severity pairs (Broders et al. 2015). Over time, some low-severity trees have achieved a high-severity rating due to progression of the disease based on repeated annual surveys, though no trees have recovered. The severity classifications used in this study reflect the ratings given to each tree in the current growth season. Trees at the DUR stand consist of low-severity ($\leq 1/3$ observed crown damage) and asymptomatic individuals, while trees at the MEF and FOX stands are composed of both low- and high-severity

infection. Since DUR did not exhibit any symptomatic trees during initial surveys in 2012, repeated annual assessments were not conducted, only for the selection of asymptomatic trees in 2014 for NSC sampling where trees at this site re-evaluated. Comparison of NSC and growth were conducted at the DUR and MEF stands, while comparisons of sapflux and gas exchange were conducted at the MEF and FOX stands.

In 2014, the mean defoliation severity rating for low- and high-severity trees was 0.6 and 2.4, respectively, at FOX, while at MEF low- and high-severity trees received ratings of 0.9 and 2.4, respectively (based on the categorical scale described above). In 2013, the year preceding measurements of sapflux and gas exchange, low- and high-severity trees at FOX exhibited ratings of 0.6 and 2.3 respectively, while, at MEF, low- and high-severity trees were rated 1.0 and 2.4 respectively. Generally, defoliation severity has gradually increased in the region since 2012 (Broders et al. 2015).

Sap flow and meteorological measurements

Transpiration was estimated using the heat ratio method (HRM), a heat pulse-based sap flow measurement technique that is well suited for resolving low flows and sap velocities up to approximately 50 cm h^{-1} (Burgess et al. 2001; Steppe et al. 2010). Sap flow probes were constructed at the University of New Hampshire using a protocol adapted from Davis et al. (2012). Probes consist of three thermocouple junctions along the length of a 1.0 mm-diameter steel needle, allowing for temperature measurements at depths of 10, 22, and 35 mm within the sapwood. Trees at sites MEF and FOX were equipped with sap flow probes in May 2014. At each site, a total of eight trees were selected for measurement. Trees were stratified into groups of four low- and high-severity for WPND based on preliminary ocular measurements of the crowns. Tree diameter at breast height (DBH, 1.3 m above ground level) ranged 21.9–55.1 cm (mean $38.0 \text{ SD} \pm 11.8 \text{ cm}$) at MEF and 27.8–43.3 cm (mean $36.0 \text{ SD} \pm 5.1$) at FOX. Two probe sets were installed at breast height on opposite sides of the tree in the north–south orientation. Prior to installation, bark and cambial tissue were carefully removed from the measurement point to ensure that probes were in direct contact with the xylem. A drill guide was placed onto the exposed area allowing for precise spacing of the sensor probes and to ensure vertical alignment. Thermocouple probes were coated in petroleum jelly and positioned at a distance 0.6 cm upstream and downstream of a 37 mm nichrome line heater ($17\text{--}20 \ \Omega$). A reflective radiant barrier was fixed around the sensors to inhibit potential heating via direct sunlight. Sensors were connected to a datalogger and multiplexor (CR1000 and AM16/32; Campbell Scientific Inc., Logan, UT, USA) powered by an external 12 V battery. A heat pulse of 2.5 s duration was sent

to the heating probe every 15-min and the change in temperature 60 s following the heat pulse was recorded for the upstream and downstream thermocouples. Measurements were conducted from mid-May through the end of August 2014. Sapwood density (ρ_d) and moisture content (m_c) were determined gravimetrically for each tree from the average of two increment core samples collected at the start and end of the measurement period. Sapwood thermal diffusivity (D) was calculated according to Vandegehuchte and Steppe (2012), for which we report a mean value of $0.0023 \text{ cm}^2 \text{ s}^{-1}$ across all core samples ($n=32$), which is close to the nominal value of $0.0025 \text{ cm}^2 \text{ s}^{-1}$ that is often used across HRM studies (Looker et al. 2016; Marshall 1958). The heat pulse velocity (V_h) is calculated as:

$$V_h = \frac{D}{x} \ln \left(\frac{v_1}{v_2} \right) 3600, \quad (1)$$

where x is the distance from the heat source (cm), and v_1 and v_2 are the changes in temperature ($^{\circ}\text{C}$) of the upstream and downstream thermocouples, respectively. Using the methodology of Burgess et al. (2001), corrections to V_h for probe misalignment and wounding were applied. Zero-flow conditions are often determined using low vapor pressure deficit (VPD) at night and/or periods of 100% relative humidity during the day (Ambrose et al. 2010; Gotsch et al. 2014). Continuous measurements of temperature and relative humidity of the canopy ($\sim 20 \text{ m}$ above ground level) were obtained on a 15-min interval using HOBO U23 Pro v2 sensors (Onset Computer Corp., Bourne, MA), from which VPD was derived. Zero-flow velocities for this study were resolved with Baseline v3.0.10 (developed by Yavor Parashkevov, Orin Lab, Duke University). Using the Baseline software, a VPD threshold was defined ($< 0.05 \text{ kPa}$) in conjunction with a 4-h nighttime interval in which V_h values remain stable. This zeroing method provides dynamic adjustment of the zero-flow rate, while allowing for nighttime transpiration and without destructive sampling at the probe location (Oishi et al. 2016). Following determination of V_h zero flow, sap flux density was then calculated as:

$$J_s = \frac{\rho_d}{\rho_s} \left(m_c + \frac{c_{dw}}{c_s} \right) V_h, \quad (2)$$

where J_s is the sap flux density ($\text{cm}^3 \text{ cm}^{-2} \text{ h}^{-1}$), ρ_s is the density of sap (1000 kg m^{-3}), c_{dw} is the specific heat capacity of the wood matrix ($1200 \text{ J kg}^{-1} \text{ K}^{-1}$), and c_s is the heat capacity of water ($4186 \text{ J kg}^{-1} \text{ K}^{-1}$). As J_s is known to decline from the outer xylem towards the sapwood, the radial profile must be accounted for to ensure robust estimates of total sap flux (Alvarado-Barrimentos et al. 2013; Gebauer et al. 2008; Wullschlegel and King 2000). A weighted average of J_s for each tree's entire sapwood area was calculated using J_s at each measurement depth and the assumed area in concentric

circles bounded by the mid-point at each thermocouple extending toward the heartwood interface. The sapwood area (cm^2) was estimated assuming a circular bole using the average sapwood thickness measured on two increment core samples for each tree. Gap filling of data was conducted on a sensor-by-sensor and tree-by-tree basis using simple linear regressions with available data. Hence, data gaps from a single depth within an individual were amended by creating a regression equation with an adjacent depth on the sample probe set. If data gaps existed in all depths within a sensor due to failure of the heating element, then gap filling was conducted via a regression equation with the probe set situated on the opposite side of the bole. All gap-fill regression equations used no less than 2000 data points (equivalent to 20.8 days of point-measurements) and an $R^2 > 0.9$ for all linear fits. Overall, sap flow data from MEF and FOX were exceptionally complete and gap filling was required for $< 3\%$ of the final data set. The average J_s of the two probe sets for each tree is reported throughout.

Leaf gas exchange

Leaf gas exchange measurements were collected during the summer of 2014 at FOX and MEF field sites using a portable photosynthesis system (LI-6400XT, Li Cor, Inc., Lincoln, NE). Measurements were conducted in July and August on warm days with low cloud cover, between the hours of 10:00 and 14:00. Twig segments containing intact fascicles were acquired from the upper $\frac{1}{3}$ of canopies (approx. 20–30 m) exposed to full light from four co-dominant trees of each WPND-severity class (the same individuals sampled for sap flux measurements) using a 12-gauge shotgun. Only twigs bearing both current-year and second-year foliage were selected for measurement, so that potential variability across segments was minimized for comparisons of needle age class. Excised twig samples were immediately submerged and cut under water to reduce the presence of embolism within the xylem (Venturas et al. 2015). Two complete fascicles consisting of ten intact needles were placed parallel to the long side of the 6.0 cm^2 cuvette for gas exchange measurement. Samples were allowed to stabilize within the chamber for approximately 2 min while holding constant the environmental parameters influencing photosynthesis. Preliminary light-response curves were conducted on a subset of needle samples to determine a light saturation point of $1000 \mu\text{mol m}^{-2} \text{ s}^{-1}$ which was used for all subsequent measurements. Other environmental parameters controlled for included the ambient CO_2 concentration (400 ppm), temperature ($26 \text{ }^{\circ}\text{C}$), relative humidity (30–40%), and airflow rate ($400 \mu\text{mol s}^{-1}$). Once photosynthesis and stomatal conductance stabilized for a given sample, five instantaneous measurements were taken over a 30 s period and the average of those measurements are reported throughout. Since

the leaf chamber assumes a uniform leaf area and needles are irregular within the cuvette, leaf area was adjusted by measuring the length and width of each fascicle with digital calipers and the total surface area calculated assuming a cylindrical shape (Johnson 1984, Eq. 2).

NSC sampling and processing

Sampling for NSC occurred at three intervals in the months of June, August, and October, at sites MEF and DUR. These two sites were selected in the interest of comparing the greatest differences in WPND severity, as MEF had exhibited chronic defoliations in the years prior to this study, while, at DUR, it was possible to identify and sample for asymptomatic trees. All trees sampled at MEF exhibited high-severity crown damage. Six mature *P. strobus* per site were selected for repeat NSC sampling, with a mean DBH of 50.3 cm (SD ± 13.8) and 53.4 cm (SD ± 14.5) at MEF and DUR, respectively. Mean live crown ratio was also similar among sampled trees between sites: 40.1% (SD ± 4.7) and 43.6% (SD ± 9.6) at MEF and DUR, respectively. These relatively high values result from an open grown habit of the individuals, where trees at MEF are generally established on the edge of a recent clear-cut, and trees at DUR are on the boundary of a wide recreational trail exposed to high light conditions. Since NSC are allocated to different storage pools over time, it was crucial to assess sugar and starch content across root, stem, and foliar tissues to derive a robust understanding of NSC throughout the tree. Carbon supply within various tissue types vary depending on the time of year that sampling occurs, such that higher NSC concentration is typically found within foliage and stems of the upper canopy early in the growing season (i.e., near the source location) and moves to storage pools within the bole and root system later in the growing season (Landhausser and Lieffers 2012). Increment core samples were obtained at two locations using a 5.15 mm increment borer: from breast height on the main stem (bole), and from a primary coarse root excavated < 1.0 m away from the trunk. Radial growth for the current-year and previous year (2015 and 2014, respectively) was assessed from core samples obtained at DBH and converted to units of basal area increment (BAI, cm²). Additionally, current-year branch segments, multiple-year branch segments (integrated 2–4 years), current-year needles, as well as second-year needles were collected. Stem samples were considered from two positions in the canopy, upper and lower, defined here as the top 1/3 and bottom 1/3 of the live crown. All stem and needle samples were acquired using a 12-ga shotgun with steel birdshot. Upon collection, samples were immediately placed on dry ice. All tissue samples were then relocated to a – 80 °C freezer until carbohydrate extractions could be performed.

Sugar and starch assays were conducted at Bates College in Lewiston, ME. Tissue samples were freeze-dried (Freezone 6; Labconco Corporation, Kansas City, MO, USA) before being ground to 20-mesh (Wiley Mini Mill; Thomas Scientific, Swedesboro, NJ, USA) and stored in 20 mL scintillation vials with airtight seals. Determination of total soluble sugar concentrations followed the protocol of Chow and Landhäusser (2004). Using this method, a ground and homogenized tissue sample is subjected to heated ethanol extraction followed by colorimetric analysis with phenol–sulfuric acid. The final extract was measured using a spectrophotometer (Spectronic 20 Genesys; Thermo Fisher Scientific, Waltham, MA, USA) at a wavelength of 490 nm with sugar concentration calculated from a standard curve of 1:1:1 glucose–fructose–galactose. For starch determination, residual tissue was subsequently solubilized by sodium hydroxide, hydrolyzed to glucose by an enzyme mixture of α -amylase and amyloglucosidase, and then measured colorimetrically using a peroxidase–glucose oxidase–*o*-dianisidine solution. Solution absorbance was read at 525 nm and starch concentration calculated based on a glucose standard.

Needle expansion

Morphological development of current-year needles was monitored at the DUR field site for the 2015 growing season. Weekly measurements of needle length were conducted on three fascicles of three white pine saplings ($n=9$) exposed to full light conditions using digital calipers. The purpose of these measurements was to determine the start and end time of the current-year needle expansion and its developmental stage relative to WPND-induced defoliation.

Analyses of physiological data

As VPD is known to be a primary driver to tree transpiration, we assessed the relationship between VPD and sap flux density as a function of disease severity. The mean daily VPD is assessed with three different metrics of sap flux density: the mean daily J_s (24 h mean), peak daily J_s (the mean J_s between the hours of 10:00–18:00), and maximum daily J_s . Non-linear curves were fit to each metric of J_s against mean daily VPD using a five-parameter log-logistic model (Ritz et al. 2015). These model fits were evaluated using a likelihood ratio test to determine if differences between severity classes were significant. To assess the impacts of defoliation on tree sap flux, continuous measurements were segmented into three discrete periods. These periods are defined as: pre-defoliation (May 21–Jun 14), during defoliation (Jun 15–Jul 14), and post-defoliation (Jul 15–Aug 27). These periods are based on repeated seasonal observations (~ 7-day interval) of the needle-cast event and supported in part by quantitative litterfall trapping measurements

(McIntire et al. 2018a) and measured spore dispersal of the WPND-associated pathogen *Lecanosticta acicola* at MEF (Wyka et al. 2018a). Differences in J_s (daily mean, peak, and maximum) were analyzed using linear mixed models, with defoliation severity class and time period evaluated as fixed effects, and sampled trees set as a random factor to account for multiple observations among individuals nested within the two sites. The mixed model fits were conducted using the R packages lme4 (Bates et al. 2015) and lmerTest (Kuznetsova et al. 2017), followed by post hoc comparisons (Tukey's method) using the emmeans package (Lenth et al. 2018). Additionally, for each site, the ratio of mean daily J_s between low- ($n=4$) and high-severity trees ($n=4$) was computed for each day of the study period, excluding days with mean VPD < 0.3 kPa. This daily J_s ratio provides a metric of water uptake for defoliated trees relative to adjacent healthier trees within each stand. Since individual low- and high-severity individuals cannot be directly paired, a site-level J_s ratio is computed for each day and sites MEF and FOX are analyzed separately. ANOVA was applied to test for the overall effect of time period and a post hoc Tukey-HSD was used to test for significant differences ($\alpha=0.05$) in the daily J_s ratio means aggregated between the pre-, during, and post-defoliation periods.

For analysis of leaf gas exchange, two dependent variables were considered: photosynthesis (A, $\mu\text{mol CO}_2 \text{ m}^{-2} \text{ s}^{-1}$), and instantaneous water use efficiency (iWUE, $\mu\text{mol CO}_2 \text{ mmol}^{-1} \text{ H}_2\text{O}$), calculated as the ratio of photosynthesis to transpiration. Since gas exchange measurements could not be conducted on the same dates for both study sites, measurements were grouped into two time periods for analysis (July vs. August), which represent the post-defoliation period. Gas exchange was measured on 8 July (MEF), 21 July (FOX), 14 August (MEF), and 21 August (FOX), during which times the July ambient VPD ranged 2.0–2.6 kPa and August ambient VPD ranged 0.9–1.0 kPa. A three-way factorial mixed model used the independent variables of needle age, defoliation severity class, and month to assess their relative impact and interactions on A and iWUE, while the individual trees for which repeat measurements were conducted was classified as a random effect within the model. Values for A met the normal distribution criteria; however, iWUE values were skewed on the lower end and a log transformation was used to meet assumptions of variance homogeneity. A post hoc analysis was conducted using linear contrast (sub-design ANOVA), testing the overall effect of one factor at a single level of another factor to determine sample means that were significantly different ($\alpha=0.05$) between disease severity within a given needle age class and sampling period for each dependent variable.

To assess the effects of time, tissue type, and WPND severity on NSC content, a repeated-measures MANOVA using a full factorial (three-way) design was conducted

using log-transformed values of sugar and starch to adhere to assumptions of normality. Significance for MANOVA was tested using the Wilk's lambda test at an alpha level of 0.05. This analysis allowed for a test of whether sugar or starch concentrations changed over time (June–Aug–Oct), differed between WPND-severity classes, differed across tissue types, and also included interactions among these three factors in a full factorial design. Thus, a within-subject factor of time is considered, while two conditions (WPND severity, tissue type) are considered between trees on the dependent variables of sugar and starch. Whole-tree NSC content (kg) were also assessed relative to the current-year and previous-year basal area increment of each tree. Measured concentrations of soluble sugar and starch were scaled to the whole-tree level using established allometric relationships of roots, foliage, and stem as a function of DBH (Furze et al. 2019; Jenkins et al. 2003). This ratio of carbohydrate content to annual woody growth ($\text{kg NSC cm}^{-2} \text{ BAI}$) provides insight to a potential trade-off between secondary growth and carbon allocation among tissue types. In this analysis, data from all sampling dates were pooled and a t test was used to infer differences within each tissue type ($\alpha=0.05$) between disease severity using log-normalized data. Statistical analyses were performed using R v3.5.1 (R Core Team 2020).

Results

Tree sap flux

Metrics of daily sap flux were highly correlated with the mean daily VPD. Trees with high-severity infection consistently exhibited lower values of daily mean J_s , daily maximum J_s , and daily peak J_s than trees of low-severity infection (Fig. 1). Likelihood ratio analyses found that the low- and high-severity model fits were significantly different from the common model fits pooling both severity classes for J_s -daily [high-severity $X^2 (1 \text{ df}) = 900.30, p < 0.01$; low-severity $X^2 (1 \text{ df}) = 835.83, p < 0.01$], J_s -peak [high-severity $X^2 (1 \text{ df}) = 1215.79, p < 0.01$; low-severity $X^2 (1 \text{ df}) = 1093.57, p < 0.01$], and J_s -max [high-severity $X^2 (1 \text{ df}) = 1122.61, p < 0.01$; low-severity $X^2 (1 \text{ df}) = 1026.15, p < 0.01$]. Each of the metrics of J_s begin to converge for the two severity classes at lower values of VPD (≤ 0.3 kPa). Mean daily J_s did not differ significantly between sites for either the low-severity [t test: $t (194) = -1.869, p = 0.631$] or high-severity trees [$t (193) = 0.732, p = 0.47$]. Maximum values of J_s were typically achieved on days where VPD exceeded 0.4 kPa (Fig. 1c). The average maximum J_s for the low- and high-severity trees above 0.4 kPa was found to be 24.7 and 19.8 $\text{cm}^3 \text{ cm}^{-2} \text{ h}^{-1}$, respectively, an apparent 20% reduction of J_s in the more diseased trees. Similarly, daily mean J_s (Fig. 1a) was found to be 21% lower and daily peak J_s

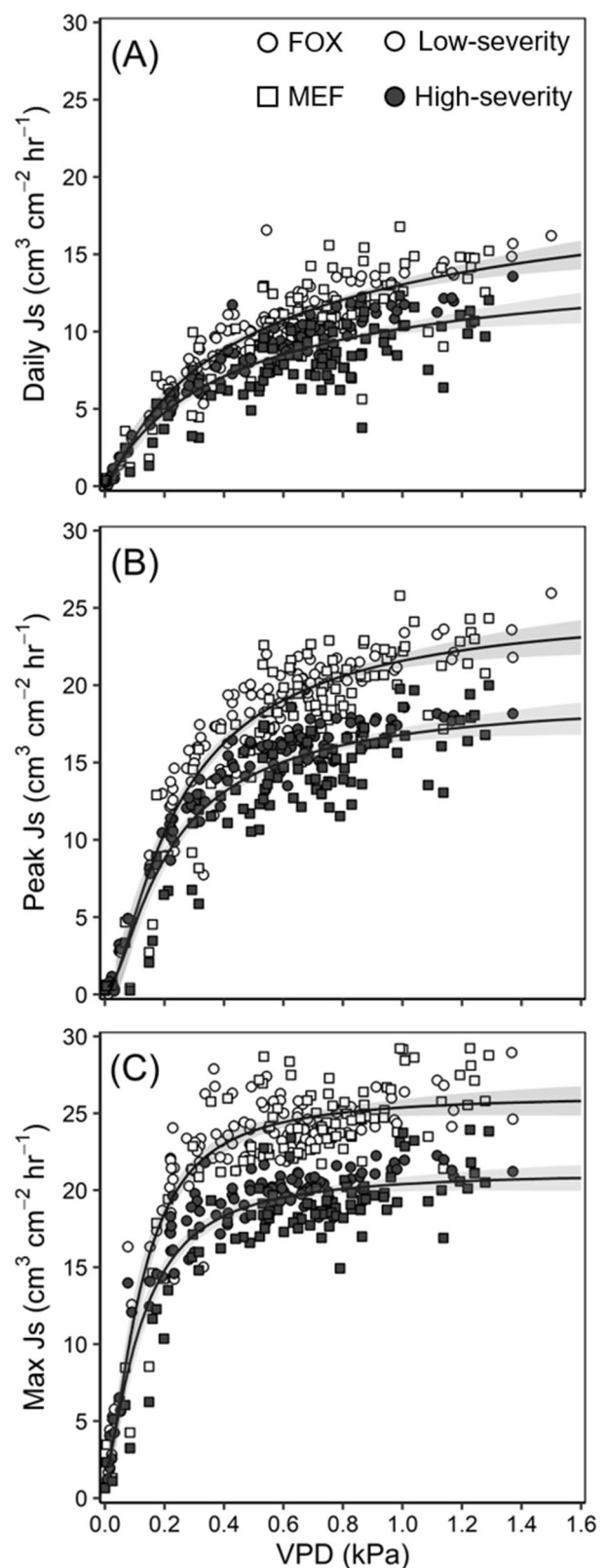
Fig. 1 Mean daily (a), peak daily (b), and maximum daily sap flux density (c) as a function of daily average VPD. Each point represents the average of individuals ($n=4$) within each severity class for a given day, circles and squares denote trees at FOX and MEF, respectively, and open and filled shapes denote the low-severity and high-severity trees respectively. Non-linear curve fits show the 95% confidence interval in the shaded ribbon for low- and high-severity trees

(Fig. 1b) 22% lower among the high-severity trees, though these differences tended to increase with VPD. Trees of either severity class exhibited nighttime transpiration when VPD remained elevated (>0.1 kPa) after sunset (Fig. 2a), and thus, daily mean values of J_s incorporate nocturnal flow rates when applicable. While high-severity trees tended to exhibit similar diurnal patterns of sap flux than their low-severity counterparts, the main differences occurred around peak hours of flow (10:00–18:00), such that high-severity trees appeared to be inhibited when VPD exceeded 2.0 kPa (Fig. 2a). On days with relatively low VPD, sap flux of low- and high-severity trees exhibited more similar diurnal patterns and the mean daily J_s ratio approached 1.0 (Fig. 2b).

We found the relative time period (pre-, during, and post-defoliation) which had a significant effect on daily mean J_s [$F(2,28) = 43.7$, $p < 0.001$], peak J_s [$F(2,28) = 19.1$, $p < 0.001$], and maximum J_s [$F(2,28) = 14.2$, $p < 0.001$]. While the mean J_s of high-severity trees was consistently reduced compared to low-severity trees, this factor did not meet our criteria for statistical significance for daily mean J_s ($p = 0.082$), peak J_s ($p = 0.059$), or maximum J_s ($p = 0.056$) (Table 1). The interaction between WPND severity and time period was not significant, suggesting that the summer defoliation event did not result in an appreciable decline in tree water flux between severity classes, in part rejecting our first hypothesis. However, the daily J_s ratio was found to differ significantly at MEF [$F(2,69) = 7.64$, $p = 0.001$] between the pre-defoliation and post-defoliation periods, indicating a reduction in sap flux density on the order of 5.3% (Fig. 3). The post-defoliation J_s ratio was reduced by 3.9% at FOX (compared to pre-defoliation), though this change over time was not significant [$F(2,75) = 3.07$, $p = 0.052$]. Interestingly, trees at FOX were found to have a lower pre-defoliation J_s ratio than compared to MEF ($p < 0.001$), suggesting that high-severity trees at the FOX site may have been more pre-disposed to infection and to the influence of chronic defoliation. During this early season pre-defoliation period, high-severity trees at FOX exhibited daily mean J_s equivalent to 76.2% the J_s of low-severity trees, while trees at MEF exhibited a J_s ratio of 87.5%.

Leaf gas exchange and expansion

A three-factor mixed model was used to test for effects of needle age, defoliation severity, month, and their interactions



for instantaneous measurements of photosynthesis (A) and $iWUE$. The significant interactive terms for A were found to be month \times needle age [$F(1,42) = 16.15$, $p < 0.001$] and

Fig. 2 Diurnal patterns of sap flux density (J_s) during 2 days of contrasting VPD on July 9 (a, b) and August 21 2014 (c, d) at MEF and FOX. Daily mean VPD for each panel is 0.9 (a), 0.5 (b), 0.2 (c), and 0.1 kPa (d). Solid line indicates VPD derived from canopy temperature and humidity on site. Open and filled symbols denote low- and high-severity trees, respectively, and shaded areas show ± 1 SE ($n=4$)

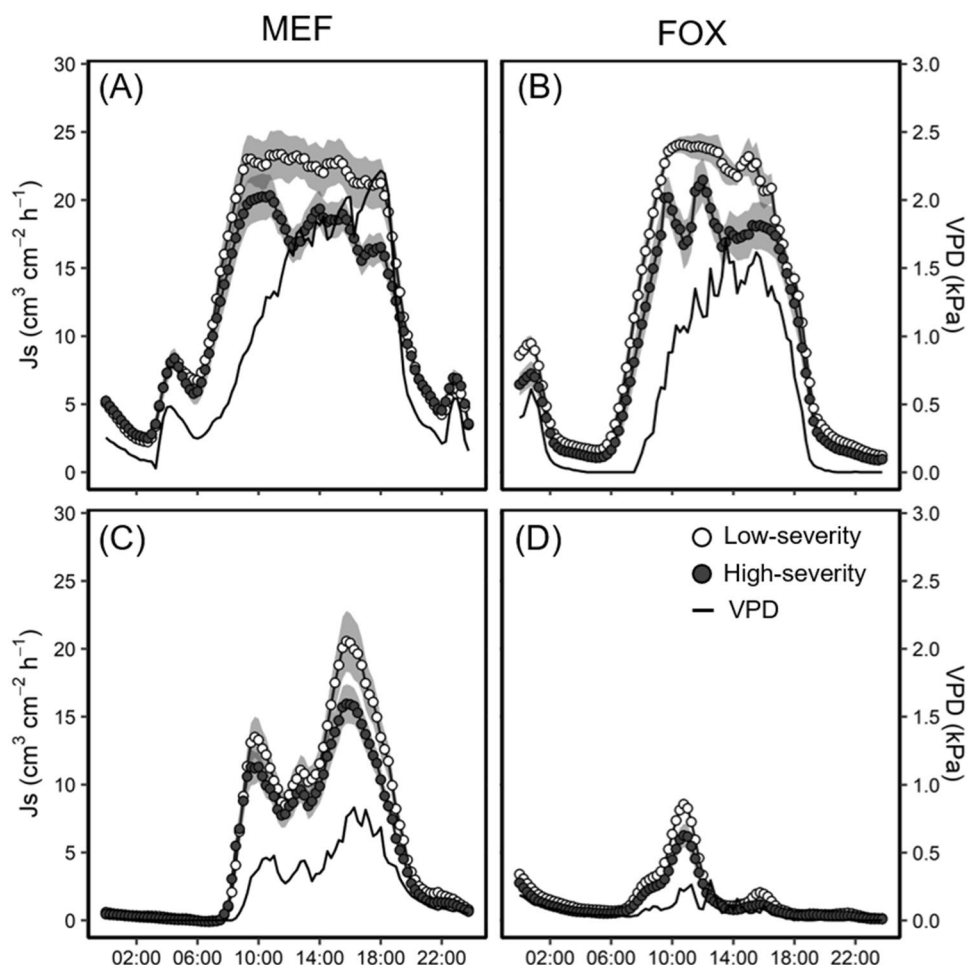


Table 1 Linear mixed model results for the effects of time (pre-, during, and post-defoliation) and defoliation severity on daily mean, daily peak (10:00–18:00), and maximum sap flux density (J_s)

Effect	Sum Sq	Mean Sq	df	F value	p value
Daily mean J_s					
Time	50.46	25.23	28	43.69	< 0.001
Severity	2.03	2.02	14	3.51	0.082
Time \times severity	0.25	0.12	28	0.21	0.810
Daily peak J_s					
Time	41.07	20.54	28	19.09	< 0.001
Severity	6.63	6.63	14	4.22	0.059
Time \times severity	0.48	0.24	28	0.15	0.859
Daily max J_s					
Time	77.73	38.87	28	14.20	< 0.001
Severity	9.84	9.84	14	4.35	0.056
Time \times severity	1.36	0.68	28	0.30	0.743

Bolded p values indicate significance at < 0.05

severity \times needle age [$F(1,42)=4.91$, $p=0.030$] (Table 2). Post hoc analyses found that photosynthesis of current-year needles during the month of July was 25.9% lower ($p=0.002$) than the mature second-year needles (pooling severity classes). Additionally, photosynthesis of current-year needles in high-severity trees increased by 24.0% from July to August ($p=0.043$) (Fig. 4b), while second-year needles among low-severity trees declined by 24.8% over this same time interval ($p=0.013$) (Fig. 4a). For iWUE only, the fixed effect of month was found to be significant [$F(1,42)=118.52$, $p<0.001$]; post hoc tests indicate iWUE of the current-year needles in August increased by 54.1% ($p<0.001$) and 78.2% ($p<0.001$) in low-severity and high-severity trees, respectively (Fig. 4c), while second-year needles exhibited an iWUE increase of 42.1% ($p<0.001$) and 63.8% ($p<0.001$) in low-severity and high-severity trees, respectively, compared to measurements conducted in the previous month of July (Fig. 4d).

Current-year fascicles at DUR were found to initiate development in early May and reach maturity by the first week of August. Growth between June 14 and July 25 advanced at a rate of 0.9 mm day^{-1} , with fully expanded

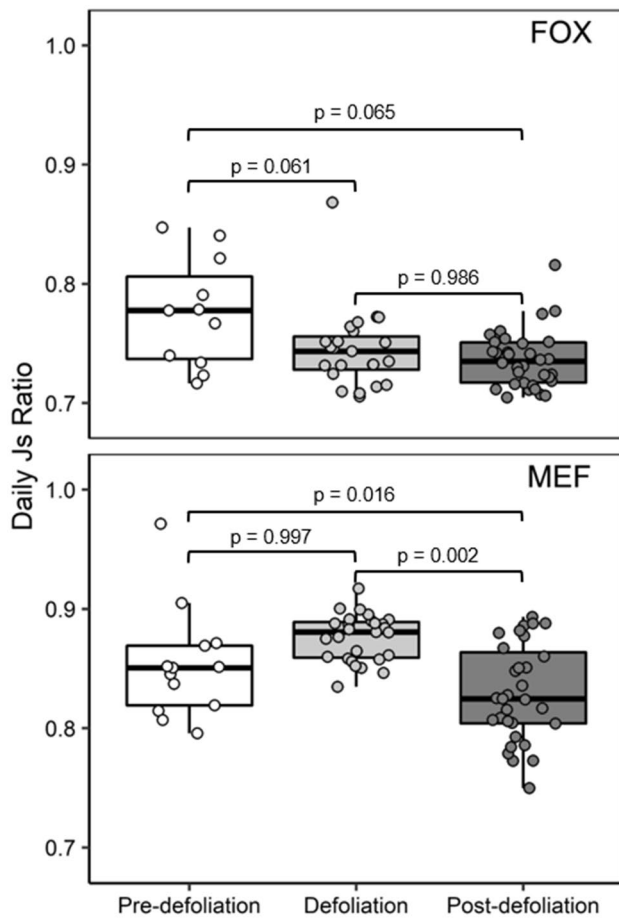


Fig. 3 Ratio of mean daily sap flux density (high-severity/low-severity trees) at each study site for the pre-defoliation (MEF $n=16$, FOX $n=14$ days), defoliation (MEF $n=29$, FOX $n=28$ days), and post-defoliation (MEF $n=39$, FOX $n=39$ days) periods. Data exclude days with mean VPD < 0.3 kPa. A difference in letters between time periods indicates a significant difference via a Tukey-HSD test, and p values between each time period are shown in connecting brackets

needles measuring 59.3 mm (SD \pm 15.0) in length. At the time of WPND-induced defoliation beginning in mid-June, current-year needles measured 23.2 mm in length; only 39% of their mature length.

Non-structural carbohydrates

Multivariate analysis of sugar concentrations (mg g^{-1}) found significant differences between trees for tissue type [$F(7,68) = 126.02, p < 0.001$], but not for disease severity [$F(1,68) = 0.15, p = 0.697$]. The within-tree interaction of time and tissue type was also significant for sugar concentration [$F(14,134) = 6.43, p < 0.001$]. Starch concentration contrasted with sugars in that the interaction of tissue \times disease severity was significant [$F(7,72) = 4.6, p < 0.001$]. The three-way interaction of time \times tissue \times disease severity was also found to be significant within trees for starch concentration [$F(14,142) = 1.70, p = 0.038$]. Within each tissue type and across sampling dates, NSC in the two disease severity classes were generally well correlated with each other, though some significant differences are noted for starch and total NSC among stem and needles tissues in July and August (Fig. 5). When considering total NSC (the sum of sugar and starch) fixed effect tests between trees found that differences in concentration were marginally significant for the interaction of tissue \times disease severity [$F(7,68) = 2.18, p = 0.047$], as well as the within trees interaction of tissue \times time [$F(14,134) = 12.42, p < 0.001$]. Full MANOVA results for sugar, starch, and total NSC by disease severity, tissue type, and time are reported in Table 3.

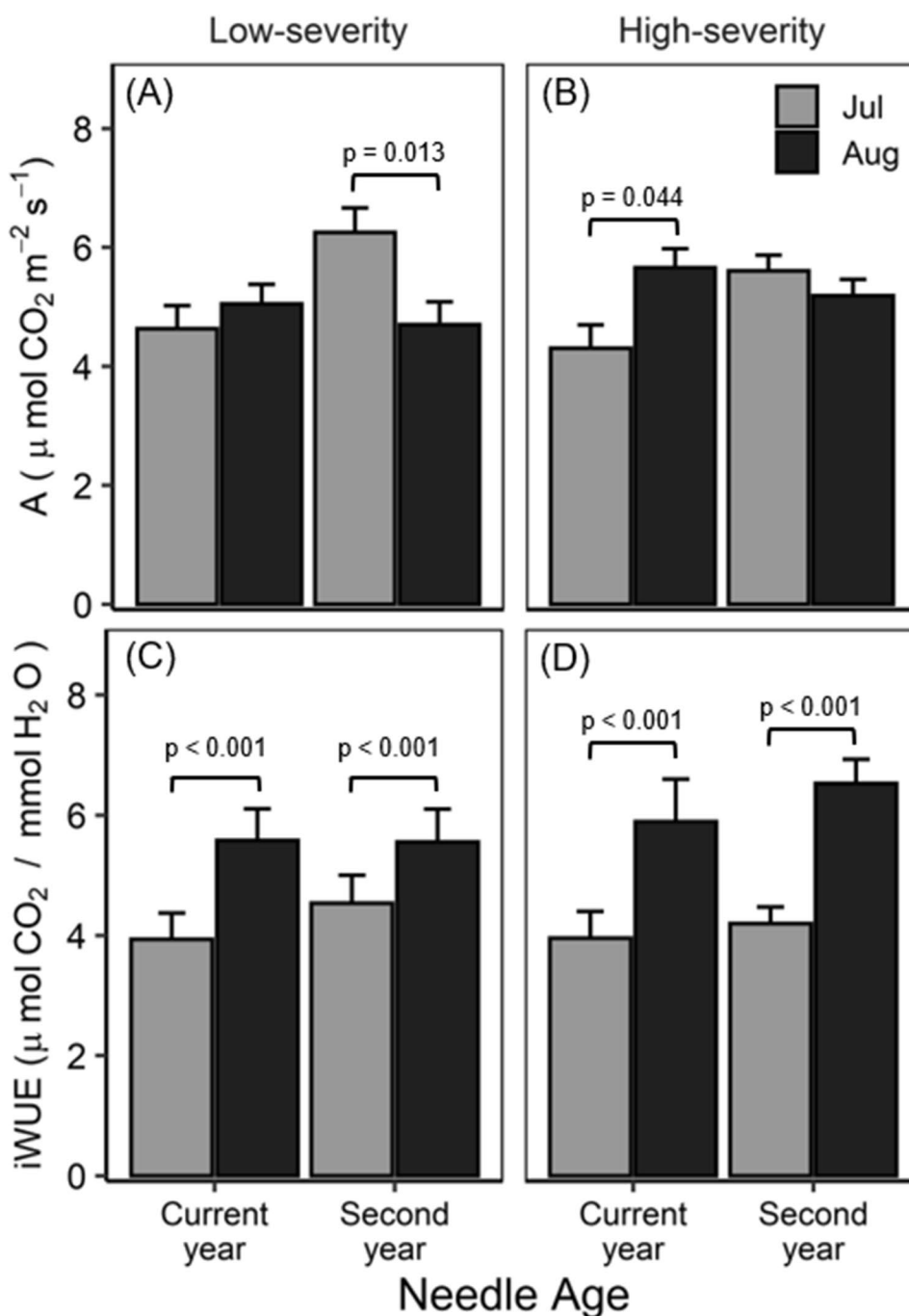
Examination of allometric-scaled NSC-to-BAI of the current-year (2015) and previous year (2014) revealed large differences between severity class for the five different tissues (Fig. 6). The mean BAI among the low-severity trees was 45.1 and 37.0 cm^2 in 2014 and 2015, respectively, while high-severity trees had a mean BAI of 20.4 and 21.9 cm^2 in 2014 and 2015. This is a difference in radial increment between high- and low-severity

Table 2 Parameters of the three-factor mixed model of A and iWUE by month (July, August), defoliation severity (high, low), and needle age class (current-year, second-year) with random effect of sampled tree nested within site (FOX, MEF)

Effect	A					iWUE				
	Sum Sq	Mean Sq	df	F value	p value	Sum Sq	Mean Sq	df	F value	p value
Age	4.41	4.41	42	5.09	0.027	1.57	1.57	42	2.03	0.162
Month	0.04	0.04	42	0.04	0.834	92.02	92.02	42	118.52	< 0.001
Severity	0.01	0.01	14	0.02	0.901	0.07	0.07	14	0.09	0.765
Age \times month	13.97	13.97	42	16.15	< 0.001	0.18	0.18	42	0.23	0.635
Age \times severity	0.20	0.20	42	0.23	0.634	0.47	0.47	42	0.61	0.440
Month \times severity	4.24	4.24	42	4.91	0.030	2.29	2.29	42	2.94	0.094
Age \times month \times severity	0.04	0.04	42	0.04	0.837	0.00	0.00	42	0.00	0.984

Bolded p values indicate significance at < 0.05

Fig. 4 Photosynthesis rates (**a**, **b**) and instantaneous water use efficiency (**c**, **d**) derived from gas exchange measurements conducted in July (grey) and August (black) by defoliation severity class and needle age pooled from sites FOX and MEF. Significant differences between means ($n = 8 \pm \text{SE}$) are determined with Tukey post hoc comparisons and indicated with brackets



trees in the previous-year and current-year of 41 and 55% respectively. The ratio of total NSC to BAI (kg cm^{-2}) was significantly higher (t test, $p < 0.05$) within high-severity trees for multi-year stem segments, current-year needles, and second-year needles when comparing the NSC-to-BAI ratio for both the current (2015) and previous year (2014). Interestingly, this ratio was also significantly elevated in high-severity individuals for root tissue when comparing the previous-year growth [$t(18) = 2.32$, $p = 0.032$], but not for the current-year growth [$t(18) = 1.79$, $p = 0.090$]. Bole

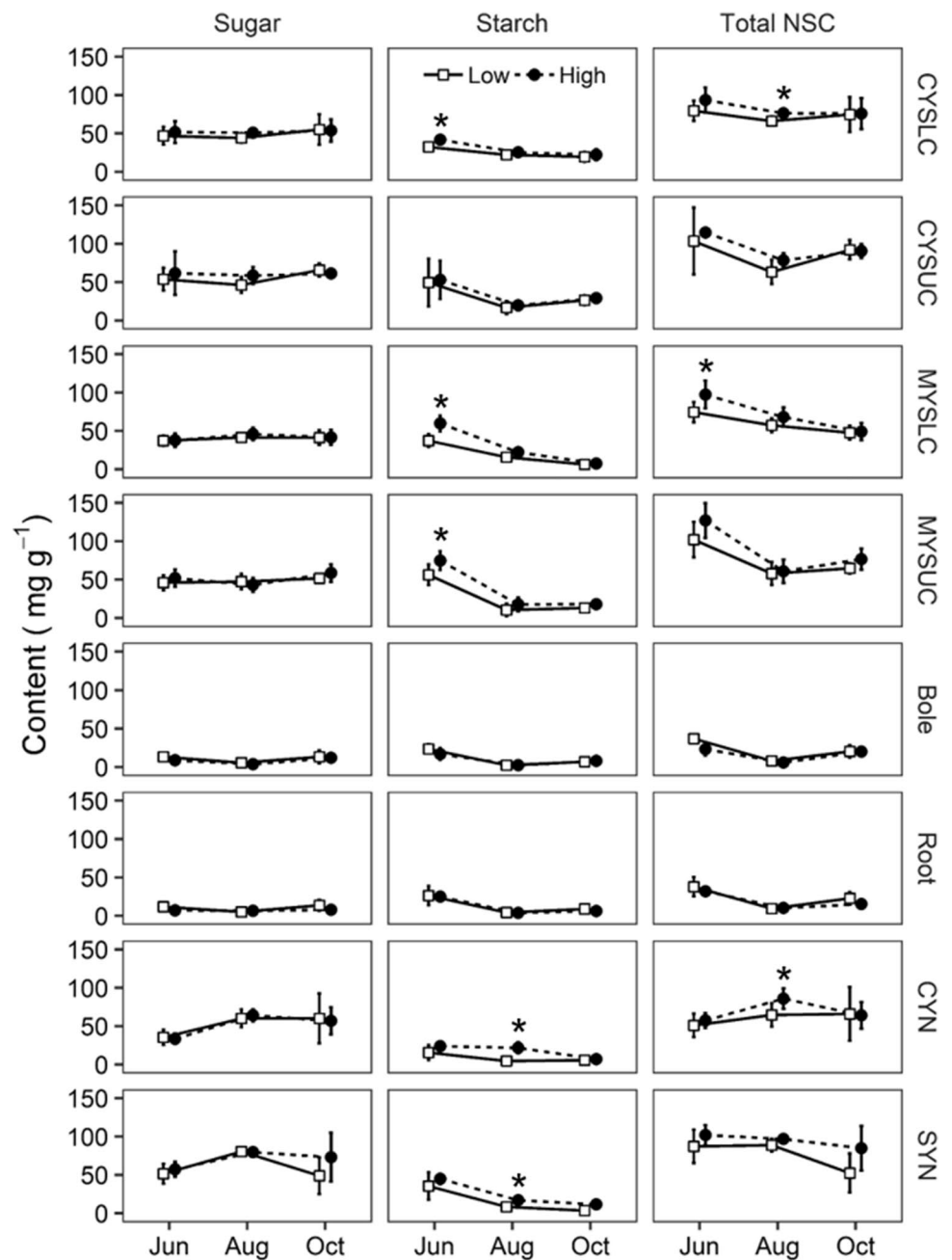
content of NSC did not differ as a function of defoliation severity class.

Discussion

Defoliated trees show decreased water use

Across both sites where sap flux was measured (FOX and MEF), high-severity *P. strobus* were found to have lower

Fig. 5 Mean starch and sugar concentration ($n=6 \pm SD$) for the asymptomatic (white squares) and high-severity WPND-infected (black circles) sites across the eight tissue types measured at DUR (asymptomatic/low severity) and MEF (high severity). Points denoted with * are significantly different ($p < 0.05$) between severity class for a given sampling period. Tissue-type guide: *CYSLC* current-year stem from the lower canopy, *CYSUC* current-year stem from the upper canopy, *MYSLC* multi-year stem from the lower canopy, *MYSUC* multi-year stem from the upper canopy, *CYN* current-year needle, *SYN* second-year needle



values of J_s throughout the 2014 growing season. On average, mean daily sap flux density of high-severity trees was 20% lower than healthy/low-severity counterparts. At low VPD (< 0.3 kPa), high-severity defoliated trees were found to have values of J_s more similar to that of low-severity individuals. In a study of defoliated *Populus tremuloides*, it was found that trees subject to leaf area reductions of 50% and 98% showed a significant increase in stomatal conductance (g_s) under low-VPD conditions (0.64 kPa) compared to control trees, but the magnitude of this increase in g_s was muted at high-VPD (1.9 kPa) (Hart et al. 2000). Similarly, defoliated *Eucalyptus globulus* demonstrated higher transpiration

rates and canopy conductance to control trees at lower values of VPD, while defoliated trees experienced a greater reduction in canopy conductance with increasing VPD compared to controls (Quentin et al. 2011). This suggests that while residual foliage may be compensating for the reduction in canopy leaf area by increasing g_s to optimize for C gain, it is not able to do so when evaporative demand is high. This is likely due to constraints induced by a reduction in leaf water potential, which may limit transpiration when VPD is high. However, others have shown an increase in branch water potential (less negative) of *P. strobus* in response to artificial defoliation of saplings (Vanderklein and Reich 2000).

Table 3 Between-subject and within-subject results of the three-factor repeated-measures MANOVA for sugar, starch, and total NSC concentrations (mg g^{-1}) comparing low-severity (DUR) and high-severity (MEF) stands

Effects	Sugar			Starch			Total NSC		
	<i>df</i>	<i>F</i>	<i>p</i> value	<i>df</i>	<i>F</i>	<i>p</i> value	<i>df</i>	<i>F</i>	<i>p</i> value
Between subjects									
All	15, 68	59.78	< 0.001	15, 72	27.20	< 0.001	15, 68	69.41	< 0.001
Intercept	1, 68	15091.51	< 0.001	1, 72	8733.09	< 0.001	1, 68	35687.90	< 0.001
Disease	1, 68	0.15	0.697	1, 72	24.81	< 0.001	1, 68	1.59	0.211
Tissue	7, 68	126.02	< 0.001	7, 72	50.69	< 0.001	7, 68	145.50	< 0.001
Tissue \times disease	7, 68	1.34	0.246	7, 72	4.60	< 0.001	7, 68	2.18	0.047
Within subjects									
All	30, 134	3.58	< 0.001	30, 142	6.17	< 0.001	30, 134	6.52	< 0.001
Time	2, 67	10.69	< 0.001	2, 71	229.50	< 0.001	2, 67	64.48	< 0.001
Time \times disease	2, 67	0.08	0.920	2, 71	2.69	0.0750	2, 67	0.25	0.782
Time \times tissue	14, 134	6.43	< 0.001	14, 142	10.75	< 0.001	14, 134	12.42	< 0.001
Time \times tissue \times disease	14, 134	1.21	0.272	14, 142	1.70	0.038	14, 134	0.99	0.471

Bolded *p* values indicate significance at < 0.05

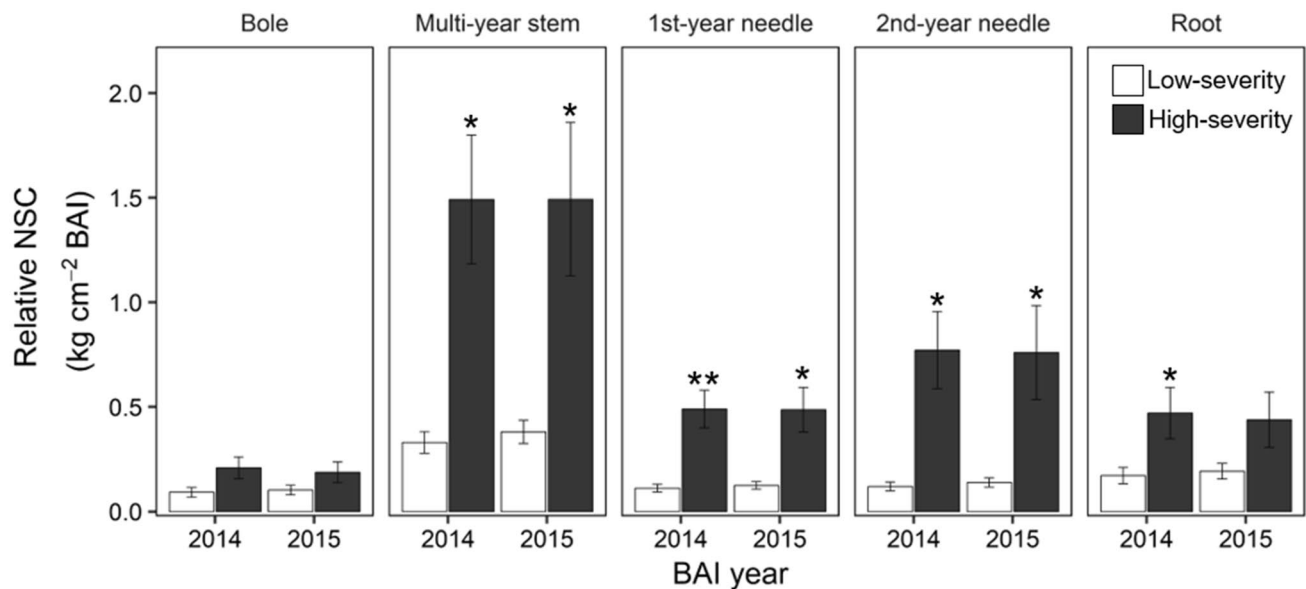


Fig. 6 The NSC content as a ratio of the previous year (2014) and current-year (2015) BAI, for each tissue type. Low-severity/asymptomatic (DUR) and high-severity (MEF) trees are denoted in white and

black bars, respectively. Means ($n = 18 \pm \text{SE}$) are significantly different at $p < 0.05$ (*) and $p < 0.001$ (**) via a paired *t* test

Physiological studies of *Pseudotsuga menziesii* defoliated by *Phaeocryptopus gaemannii* have shown significant reductions in branch leaf specific conductance as a result of leaf area reduction (Manter and Kavanagh 2003). Similarly, *Arceuthobium tsugense* infection of *Tsuga heteriohylla* has been found to induce substantial reductions in canopy leaf area, resulting in reduced sapwood area, declines in whole-tree water use, and lower hydraulic conductivity (Meinzer et al. 2004). Though it is well established that VPD, leaf-stem water potential, and conductance are tightly linked to

transpiration (Simonin et al. 2015), it is interesting to note the feedback effect in which defoliation appears to alter the influence of VPD on whole tree water use. At high midday VPD, high-severity *P. strobus* appear inhibited, showing a marked reduction in J_s when VPD exceeds 2.0 kPa, while low-severity trees plateau and maintain relatively high values of midday J_s (Fig. 2a).

Despite significant differences in J_s between severity classes as a function of VPD, the defoliation event which started in mid-June did not influence a substantial further

decline in the water use of high-severity trees, as the J_s ratio differed between the pre- and post-defoliation periods by only 3.9% and 5.3% at FOX and MEF, respectively. This suggests that the initial defoliation has long-term consequences for tree water use, since it is known that trees sampled at both sites have suffered from chronic pathogen-induced defoliation since at least 2012, 2 years prior to this study. As healthy *P. strobus* typically retain 2–3 years of foliage throughout the growing season, severely defoliated trees often possess only current-year foliage from July to the subsequent May when the new cohort of needles begins to form. Given chronic annual defoliations, high-severity trees exhibit thinned crowns for multiple years as the older mature foliage is continually reduced. Therefore, the already thinned crowns of diseased trees at the start of a growing season are likely a more important factor than the subsequent defoliation within a given year in terms of tree water use within stands that have been infected previously. All sampled trees were in the co-dominant canopy stratum; thus, it is unlikely that overstory shading played a role in the reduced sap flux rates measured in the high-severity trees. It is also plausible that the impacts of defoliation are subtle due to the concurrent expansion of the current-year foliage during the time at which mature second- and third-year needles are being cast. During the month of June, the current-year needles are only 39% of full expansion at the start of the defoliation event. Thus, gross photosynthesis (and transpiration) would be expected to increase as development of current-year needles progress, despite the loss of much of the mature foliage. As the current-year needles continue to develop post-defoliation, they act to offset the C lost from second- and third-year needles.

Regulation of gas exchange in residual needles

Analyses of photosynthesis (A) revealed significant effects of needle age over time within both severity classes (Table 2). Conifer foliar expansion occurs over a time span of several months (Cuny et al. 2012; Rossi et al. 2009; Sampson et al. 2003), which differs from deciduous broadleaf species that typically expand and mature rapidly. Second-year needles were found to have significantly higher rates of A than current-year needles during the month of July (Fig. 4); however, by the time current-year foliage reached full expansion in August, there was no difference in assimilation rates between age classes. Our linear mixed model did not find a consistent effect of defoliation severity on gas exchange across all age classes and time periods, though it is worth noting that the interaction of defoliation severity over time was found to be significant, indicating a trend of A increasing over time among trees of high defoliation severity. This finding suggests a compensation response occurring within high-severity crowns, in which residual needles of high-severity

trees are upregulating photosynthesis due to a lack of mature foliage later in the season. Photosynthesis of current-year foliage within high-severity trees was significantly higher than that of low-severity trees in the month of August. We found the opposite response within the second-year foliage of low-severity trees—a significant downregulation of photosynthesis in August, presumably due to the fact that the current-year foliage is able to contribute a higher proportion of gross carbon assimilation now that the needles have reached full expansion. This compensatory response has been confirmed in other *Pinus* species subjected to defoliation (Eyles et al. 2011).

The effects of month on iWUE were highly significant, increasing between July and August across both needle age classes and defoliation severity classes (Table 2, Fig. 4c, d). This effect may in part explain the unexpectedly subtle decline in post-defoliation sap flux, since it appears that as the growing season progresses, trees are able to use less water through transpiration per unit carbon assimilated.

Dynamics of NSC allocation and storage

Despite the substantial reduction in total leaf area and similar leaf-level C assimilation rates, we observed that severely defoliated trees are storing NSC at nearly the same concentration across tissue types as low-severity trees (Fig. 5). With the exception of starch content in the month of August, we observed no differences in NSC concentrations between the current-year and second-year needles, contrary to the findings of Li et al. (2009) and Yan et al. (2012). Additionally, we found only a modest effect of disease severity between tissue types' total NSC (Table 3). This finding is interesting in light of clear declines in basal area increment due to WPND-induced defoliations since the onset of outbreaks in the northeastern US. McIntire et al. (2018a) report declines in BAI that ranged from 25 to 73%, with post-outbreak declines at FOX and MEF of 35% and 26%, respectively. However, research has shown that stored NSC and growth are not always tightly linked. In a foliar fungal disease similar to the WPND complex, Douglas-fir (*Pseudotsuga menziesii*) defoliation via Swiss needle-cast (*Phaeocryptopus gaeumannii*) was found to significantly reduce wood growth ahead of observed declines in NSC reserves (Saffell et al. 2014a, b), suggesting that trees will store NSC in times of defoliation stress to allocate towards new foliar material, maintenance respiration, and defense, at the expense of radial growth. Other studies have demonstrated similar results in which a reduction in wood growth is reported with no change in NSC concentration of defoliated trees, including defoliation of *Pinus pinaster* by *Thaumetopoea pityocampa* (Jacquet et al. 2013) and repeated artificial defoliation of *Pinus radiata* genotypes (Gómez-Gallego et al. 2020).

In some cases, the time elapsed since the initial defoliation event can influence NSC storage within various tissue pools. Several studies have reported only short-term declines in NSC concentration, with no long-term difference in sugar or starch concentrations between healthy and defoliated trees (Gómez-Gallego et al. 2020; Palacio et al. 2008, 2012; Puri et al. 2015b; Saffell et al. 2014a, b; Wiley et al. 2013). It is plausible that the impacts of WPND have yet to reach a critical threshold of reduced gross carbon assimilation, at which point it may be expected to observe declines in stored NSC. This assertion is supported in part by the low levels of observed mortality attributed to WPND (Constanza et al. 2018). As depletion of NSC is hypothesized as a pathway of plant mortality (McDowell 2011; McDowell et al. 2008), it is reasonable to expect low soluble sugar and starch stores just prior to tree death (Dickman et al. 2015). Interestingly, we found that starch concentration was significantly *higher* among trees of high severity, contrary to depleted reserves as we had expected to observe following multiple years of defoliation. However, this was not the case for sugar concentrations, nor statistically significant for each tissue type when considering total NSC.

The literature on the effects of defoliation on NSC concentration in trees is mixed; there are many examples in which a decline or increase in NSC is found to occur in some tissues types and not others, only at certain times in the growing season, in conjunction with other stressors, and at variable levels of relative defoliation intensity (Deslauriers et al. 2015; Handa et al. 2005; Li et al. 2002; Palacio et al. 2008; Piper et al. 2015; Puri et al. 2015b). Each of these studies support the finding that the relative importance of stem growth is a lower priority than the carbon requirement for other physiological processes within trees, though the order hierarchy of such processes is complex and generally unresolved.

Alternatively, the defoliation itself may not induce carbon limitation, such that growth is limited by factors other than available carbon. The influence of shaded needles in the lower crown of conifer species has been known to serve as nutrient storage, which may be resorbed and utilized by newer foliage in the event of a defoliation (Hirose 2012; Millard and Grelet 2010). In a regional assessment of WPND defoliation that utilizes the same sites as this study (DUR, FOX, and MEF), it was found that defoliated *P. strobus* foliage contained higher levels of nitrogen in the month of June than in October, but June nitrogen content being lower than that of reported values for green foliage, implying that at least a partial resorption had occurred (McIntire et al. 2018a). Therefore, trees subject to pathogenic defoliations may be more nutrient-limited than carbon-limited.

When considering the secondary growth of each tree via the ratio of total sugar and starch content to current-year and previous-year stem basal area increment (kg NSC cm^{-2}

BAI), we found significant differences between trees of high and low severity across needle tissues (Fig. 6), suggesting that diseased trees may be prioritizing NSC for storage to be used in the following years to perpetually bolster lost foliage. We have shown that mature *P. strobus* have the ability to survive consecutive years of defoliation without a significant effect in total NSC despite reductions in secondary growth. However, this may not be the case for younger trees of seedling and sapling size classes, in which growth is more important for ensuring survival. As this study did not address carbohydrate dynamics of young trees, further research will be necessary to evaluate the long-term survival and competitiveness of *P. strobus* regeneration within stands affected by WPND.

Conclusions

Pathogen-induced defoliation of mature *P. strobus* caused by fungi associated with WPND has important physiological consequences for seasonal water and carbon dynamics. Trees that had been defoliated for multiple years prior to this study were found to have significantly reduced transpiration rates, with mean daily sap flux density 20% less than that of healthy/low-severity individuals. We found that high-severity trees reduced sap flux density an additional ~5% relative to low-severity trees following the 2014 defoliation event. Trees infected for multiple years of summer defoliations have not yet been observed returning to a healthy state with crowns retaining multiple years of mature foliage. The increase in litterfall to infected stands has cascading influences on the flux of nutrients to the forest floor, as litter deposited in the months of June and July has significantly higher nitrogen content than litter that is released during natural needle senescence in October (McIntire et al. 2018a). This may alter decomposition and soil microbial activity and, consequently, impact the availability of tree nutrients, both for mature *P. strobus* and co-occurring species such as *Quercus rubra* and *Tsuga canadensis* which are often in competition. A thicker litter layer due to chronic defoliations may also impact the ability of precipitation to infiltrate the soil and alter runoff (Neris et al. 2013). While a reduction in sap flux measured among diseased trees could represent greater soil water availability, the reduction in canopy leaf area also modifies the light regime of the understory, such that advanced regeneration could benefit and, perhaps, represent increased competition for resources.

There is evidence that residual current-year needles of diseased trees may partially compensate for the loss of foliar area by upregulating photosynthesis in the late growing season. However, there was a clear difference in C allocation to radial growth between high- and low-severity trees sampled in this study, with severely defoliated growing

55% less basal area than low-severity trees in 2015. Despite clear reductions in water use and C allocation to secondary growth, we found limited effect on total NSC across tissue types throughout the 2015 growing season between our high- and low-severity stand. These findings suggest that mature diseased trees may be prioritizing NSC storage over radial growth and the defoliations caused by WPND to date have not stressed trees to the point at which stored NSC is needed to sustain metabolic processes for survival. Additionally, there exists the possibility that reduced growth resulted due to a scarcity of available nitrogen, lost from the lower crown through repeated summer defoliations. In this case, C-limitation may not occur, yet nutrient limitation may be responsible for declines in secondary growth. Further research is necessary to parse out the precise mechanism of growth reductions, and additional attention should be given to the productivity and survivability of *P. strobus* subject to chronic pathogenic defoliation, particularly among juvenile and regenerating stands.

Author contribution statement Conceptualization: CM, IM, BH, and HA. Field measurements: CM, BH, and IM. Lab processing of carbohydrates: BH, and ED. Data analysis: CM. Supervision: IM, HA, BH, and MV. Writing: CM. All authors read and commented on this manuscript.

Acknowledgements This research was funded by USDA Forest Health Protection NA Grant 15DG-11420004-150 and the New Hampshire Agricultural Experiment Station. We are grateful for the cooperation of the USFS Northern Research Station, the Massabesic Experimental Forest, the Caroline A. Fox Research and Demonstration Forest, and the UNH Office of Woodlands and Natural Areas. The authors are also thankful for the field assistance from Steve Eisenhaure, Stephen Wyka, Connor Brenton, Sydney Snelling, and Katerine Sinacore.

Compliance with ethical standards

Conflict of interest The authors have no conflict of interest to declare.

Ethical statement This manuscript is not currently being considered for publication in another journal.

References

- Alvarado-Barrientos MS, Hernández-Santana V, Asbjornsen H (2013) Variability of the radial profile of sap velocity in *Pinus patula* from contrasting stands within the seasonal cloud forest zone of Veracruz, Mexico. *Agric For Meteorol* 168:108–119
- Ambrose AR, Sillett SC, Koch GW, Van Pelt R, Antoine ME, Dawson TE (2010) Effects of height on treetop transpiration and stomatal conductance in coast redwood (*Sequoia sempervirens*). *Tree Physiol* 30(10):1260–1272
- Bates D, Maechler M, Bolker B, Walker S, Christensen RHB, Singmann H, Dai B, Scheipl F, Grothendieck G, Green P (2018) Package ‘lme4’, version, 1, 17
- Broders K, Munck I, Wyka S, Iriarte G, Beaudoin E (2015) Characterization of fungal pathogens associated with White Pine Needle Damage (WPND) in Northeastern North America. *Forests* 6(11):4088–4104
- Burgess SS, Adams MA, Turner NC, Beverly CR, Ong CK, Khan AA, Bleby TM (2001) An improved heat pulse method to measure low and reverse rates of sap flow in woody plants. *Tree Physiol* 21(9):589–598
- Costanza KKL, Whitney TD, McIntire CD, Livingston WH, Gandhi KJK (2018) Forest ecology and management. A synthesis of emerging health issues of eastern white pine (*Pinus strobus*) in eastern North America. *For Ecol Manag* 423:3–17
- Cuny HE, Rathgeber CBK, Lebourgeois F, Fortin M, Fournier M (2012) Life strategies in intra-annual dynamics of wood formation: example of three conifer species in a temperate forest in north-east France. *Tree Physiol* 32(5):612–625
- Damascos MA, Ronquim CC, Henrique C, Assis B (2005) Gas exchange and plant growth after defoliation on *Leandra lacunosa*, a Cerrado Woody species with continuous leaf production. *Braz Arch Biol Technol* 48:967–974
- Davis TW, Kuo C-M, Liang X, Yu P-S (2012) Sap flow sensors: construction, quality control and comparison. *Sensors* 12(12):954–971
- Deslauriers A, Caron L, Rossi S (2015) Carbon allocation during defoliation: testing a defense-growth trade-off in balsam fir. *Front Plant Sci* 6:1–13
- Dickman LT, Mcdowell NG, Sevanto S, Pangle RE, Pockman WT (2015) Carbohydrate dynamics and mortality in a piñon-juniper woodland under three future precipitation scenarios. *Plant Cell Environ* 38:729–739
- Dietze MC, Sala A, Carbone MS, Czimczik CI, Mantooth JA, Richardson AD, Vargas R (2014) Nonstructural carbon in woody plants. *Annu Rev Plant Biol* 65(1):667–687
- Eyles A, Smith D, Pinkard EA, Smith I, Corkrey R, Elms S, Beadle C, Mohammed C (2011) Photosynthetic responses of field-grown *Pinus radiata* trees to artificial and aphid-induced defoliation. *Tree Physiol* 31:592–603
- Furze ME, Huggett BA, Aubrecht DM, Stolz CD, Carbone MS, Richardson AD (2019) Whole-tree nonstructural carbohydrate storage and seasonal dynamics in five temperate species. *New Phytol* 221:1466–1477
- Gebauer T, Horna V, Leuschner C (2008) Variability in radial sap flux density patterns and sapwood area among seven co-occurring temperate broad-leaved tree species. *Tree Physiol* 28(12):1821–1830
- Gómez-Gallego M, Williams N, Leuzinger S, Scott PM, Bader MK (2020) No carbon limitation after lower crown loss in *Pinus radiata*. *Ann Bot* 125:955–967
- Gotsch SG, Asbjornsen H, Holwerda F, Goldsmith GR, Weintraub AE, Dawson TE (2014) Foggy days and dry nights determine crown-level water balance in a seasonal tropical montane cloud forest. *Plant Cell Environ* 37(1):261–272
- Handa I, Korner C, Hattenschwiler S (2005) A test of the treeline carbon limitation hypothesis by in situ CO₂ enrichment and defoliation. *Ecology* 86(5):1288–1300
- Hart M, Hogg EH, Lieffers VJ (2000) Enhanced water relations of residual foliage following defoliation in *Populus tremuloides*. *Can J Bot* 78(5):583–590
- Hirose T (2012) Leaf-level nitrogen use efficiency: definition and importance. *Oecologia* 169:591–597
- Hudgeons JL, Knutson AE, Heinz KM, Deloach CJ, Dudley TL, Pattison RR, Kiniry JR (2007) Defoliation by introduced *Diorhabda elongata* leaf beetles (Coleoptera: Chrysomelidae) reduces carbohydrate reserves and regrowth of *Tamarix* (Tamaricaceae). *Biol Control* 43:213–221
- Hultine KR (2010) Sap-flux scaled transpiration by tamarisk (*Tamarix spp.*) before, during and after episodic defoliation by the

- Saltcedar Leaf Beetle (*Diorhabda carinulata*). *Agric For Meteorol* 150:1467–1475
- Jacquet J, Bosc A, O'Grady AP, Jactel H (2013) Pine growth response to processionary moth defoliation across a 40-year chronosequence. *For Ecol Manag* 293:29–38
- Jacquet J, Bosc A, Grady AO, Jactel H (2014) Combined effects of defoliation and water stress on pine growth and non-structural carbohydrates. *Tree Physiol* 34:1–10
- Jenkins JC, Chojnacky DC, Heath LS, Birdsey RA (2003) Comprehensive database of diameter-based biomass regressions for North American tree species. In: USDA Forest Service, General Technical Report NE-319, pp 1–48
- Johnson JOND (1984) A rapid technique for estimating total surface area of pine needles. *For Sci* 30(4):913–921
- Kuznetsova A, Brockhoff PB, Christensen RHB (2017) lmerTest package: tests in linear mixed effects models. *J Stat Softw* 82(13):1–26
- Landhausser SM, Lieffers VJ (2012) Defoliation increases risk of carbon starvation in root systems of mature aspen. *Trees* 26:653–661
- Lenth R, Singmann H, Love J, Buerkner P, Herve M (2018) Emmeans: estimated marginal means, aka least-squares means. R package version 1(1):3
- Li M, Hoch G, Körner C (2002) Source/sink removal affects mobile carbohydrates in *Pinus cembra* at the Swiss treeline. *Trees* 16(4–5):331–337
- Li M, Kong G, Zhu J (2009) Vertical and leaf-age-related variations of nonstructural carbohydrates in two alpine timberline species, southeastern Tibetan Plateau. *J For Res* 14(4):229–235
- Looker N, Martin J, Jencso K, Hu J (2016) Contribution of sapwood traits to uncertainty in conifer sap flow as estimated with the heat-ratio method. *Agric For Meteorol* 223:60–71
- Marshall DC (1958) Measurement of sap flow in conifers by heat transport. *Plant Physiol* 33(6):385–396
- McDowell NG (2011) Mechanisms linking drought, hydraulics, carbon metabolism, and vegetation mortality. *Plant Physiol* 155(3):1051–1059
- McDowell N, Pockman WT, Allen CD, Breshears DD, Cobb N, Kolb T, Plaut J, Sperry J, West A, Williams DG, Yezzer EA (2008) Mechanisms of plant survival and mortality during drought: why do some plants survive while others succumb to drought? *New Phytol* 178(4):719–739
- McIntire CD, Munck IA, Ducey MJ, Asbjornsen H (2018) Thinning treatments reduce severity of foliar pathogens in eastern white pine. *For Ecol Manag* 423:106–113
- McIntire C, Munck I, Vadeboncoeur MA, Livingston W, Asbjornsen H (2018) Impacts of White Pine Needle Damage on seasonal litterfall dynamics and wood growth of eastern white pine (*Pinus strobus*) in New England. *For Ecol Manag* 423:27–36
- Meinzer FC, Grantz DA (1991) Coordination of stomatal, hydraulic, and canopy boundary layer properties: do stomata balance conductances by measuring transpiration? *Physiol Plant* 83(2):324–329
- Meinzer FC, Woodruff DR, Shaw DC (2004) Integrated responses of hydraulic architecture, water and carbon relations of western hemlock to dwarf mistletoe infection. *Plant Cell Environ* 27:937–946
- Millard P, Grelet GA (2010) Nitrogen storage and remobilization by trees: ecophysiological relevance in a changing world. *Tree Physiol* 30(9):1083–1095
- Munck IA, Ostrofsky WD, Burns B (2012) Eastern White Pine Needle Damage. In: USDA Forest Service Northeastern Area State and Private Forestry (NA-PR-01-11), pp 1–4
- Neris J, Tejedor M, Rodríguez M, Fuentes J, Jimenez C (2013) Effect of forestfloor characteristics on water repellency, infiltration, runoff and soil loss in Andisols of Tenerife (Canary Islands, Spain). *Cantena* 108:50–57
- Oishi AC, Hawthorne DA, Oren R (2016) ScienceDirect Baseline: an open-source, interactive tool for processing sap flux data from thermal dissipation probes. *SoftwareX* 5:139–143
- Palacio S, Hester AJ, Maestro M, Millard P (2008) Browsed *Betula pubescens* trees are not carbon-limited. *Funct Ecol* 22(5):808–815
- Palacio S, Hernández R, Maestro-Martínez M, Camarero J (2012) Fast replenishment of initial carbon stores after defoliation by the pine processionary moth and its relationship to the re-growth ability of trees. *Trees Struct Funct* 26(5):1627–1640
- Pataki DE, Oren R, Phillips N (1998) Responses of sap flux and stomatal conductance of *Pinus taeda* L. trees to stepwise reductions in leaf area. *J Exp Bot* 49(322):871–878
- Piper FI, Gundale MJ, Fajardo A (2015) Extreme defoliation reduces tree growth but not C and N storage in a winter-deciduous species. *Ann Bot* 115(7):1093–1103
- Puri E, Hoch G, Körner C (2015a) Defoliation reduces growth but not carbon reserves in Mediterranean *Pinus pinaster* trees. *Trees* 29(4):1187–1196
- Puri E, Hoch G, Körner C (2015b) Defoliation reduces growth but not carbon reserves in Mediterranean *Pinus pinaster* trees. *Trees* 29(4):1187–1196
- Quentin AG, O'Grady AP, Beadle CL, Worledge D, Pinkard EA (2011) Responses of transpiration and canopy conductance to partial defoliation of Eucalyptus globulus trees. *Agric For Meteorol* 151(3):356–364
- R Core Team (2020) R: A language and environment for statistical computing. R Foundation for Statistical Computing, Vienna, Austria. <https://www.R-project.org/>
- Reich PB, Walters MB, Krause SC, Vanderklein DW, Raffe KF, Tabone T (1993) Growth, nutrition and gas exchange of *Pinus resinosa* following artificial defoliation. *Trees* 7(2):67–77
- Richardson AD, Carbone MS, Huggett BA, Furze ME, Czimeczik CI, Walker JC, Xu X, Schaberg PG, Murakami P (2015) Distribution and mixing of old and new nonstructural carbon in two temperate trees. *New Phytol* 206(2):590–597
- Ritz C, Baty F, Streibig JC, Gerhard D (2015) Dose-response analysis using R. *PLoS ONE* 10(12):1–13
- Rossi S, Rathgeber CB, Deslauriers A (2009) Comparing needle and shoot phenology with xylem development on three conifer species in Italy. *Ann For Sci* 66(2):206–213
- Saffell BJ, Meinzer FC, Voelker SL, Shaw DC, Brooks JR, Lachenbruch B, McKay J (2014a) Tree-ring stable isotopes record the impact of a foliar fungal pathogen on CO₂ assimilation and growth in Douglas-fir. *Plant Cell Environ* 37:1536–1547
- Saffell BJ, Meinzer FC, Woodruff DR, Shaw DC, Voelker SL, Lachenbruch B, Falk K (2014b) Seasonal carbohydrate dynamics and growth in Douglas-fir trees experiencing chronic, fungal-mediated reduction in functional leaf area. *Tree Physiol* 34(3):218–228
- Sampson DA, Albaugh TJ, Johnsen KH, Allen HL, Zarnoch SJ (2003) Monthly leaf area index estimates from point-in-time measurements and needle phenology for *Pinus taeda*. *Can J For Res* 33(12):2477–2490
- Simonin KA, Burns E, Choat B, Barbour MM, Dawson TE, Franks PJ (2015) Increasing leaf hydraulic conductance with transpiration rate minimizes the water potential drawdown from stem to leaf. *J Exp Bot* 66(5):1303–1315
- Steppe K, De Pauw DJW, Doody TM, Teskey RO (2010) A comparison of sap flux density using thermal dissipation, heat pulse velocity and heat field deformation methods. *Agric For Meteorol* 150(7–8):1046–1056
- Thomas AH, Sadras VO (2001) The capture and gratuitous disposal of resources by plants. *Br Ecol Soc* 15(1):3–12
- Vandegehuchte MW, Steppe K (2012) Improving sap flux density measurements by correctly determining thermal diffusivity, differentiating between bound and unbound water. *Tree Physiol* 32(7):930–942

- Venturas MD, Mackinnon ED, Jacobsen AL, Pratt RB (2015) Excising stem samples underwater at native tension does not induce xylem cavitation. *Plant Cell Environ* 38(6):1060–1068
- Wargo PM, Minocha R, Wong BL, Long RP, Horsley SB, Hall TJ (2002) Measuring changes in stress and vitality indicators in limed sugar maple on the Allegheny Plateau in north-central Pennsylvania. *Can J For Res* 641:629–641
- Wiley E, Helliker B (2012) A re-evaluation of carbon storage in trees lends greater support for carbon limitation to growth. *New Phytol* 195(2):285–289
- Wiley E, Huepenbecker S, Casper BB, Helliker BR (2013) The effects of defoliation on carbon allocation: can carbon limitation reduce growth in favour of storage? *Tree Physiol* 33:1216–1228
- Wiley E, Casper BB, Helliker BR (2016) Recovery following defoliation involves shifts in allocation that favour storage and reproduction over radial growth in black oak. *J Ecol* 105:412
- Williams JP, Hanavan RP, Rock BN, Minocha SC, Linder E (2016) Influence of Hemlock Woolly Adelgid infestation on the physiological and reflectance characteristics of Eastern Hemlock. *Can J For Res* 426:410–426
- Wullschlegel SD, King AW (2000) Radial variation in sap velocity as a function of stem diameter and sapwood thickness in yellow-poplar trees. *Tree Physiol* 20(8):511–518
- Wyka SA, Smith C, Munck IA, Rock BN, Ziniti BL, Broders K (2017) Emergence of White Pine Needle Damage (WPND) in the north-eastern US is associated with changes in pathogen pressure in response to climate change. *Glob Change Biol* 23(1):392–405
- Wyka SA, Mcintire CD, Smith C, Munck IA, Rock BN, Asbjornsen H, Broders KD (2018a) Effect of climatic variables on abundance and dispersal of *Lecanosticta acicola* spores and impact of defoliation on eastern white pine. *Phytopathology* 108(3):374–383
- Wyka SA, Munck IA, Brazeo NJ, Broders KD (2018b) Response of eastern white pine and associated foliar, blister rust, canker and root rot pathogens to climate change. *For Ecol Manag* 238:18–26
- Yan C, Han S, Zhou Y, Wang C, Dai G, Xiao W, Li M-H (2012) Needle-age related variability in nitrogen, mobile carbohydrates, and $\delta^{13}\text{C}$ within *Pinus koraiensis* tree crowns. *PLoS ONE* 7(4):16–19

Publisher's Note Springer Nature remains neutral with regard to jurisdictional claims in published maps and institutional affiliations.